

# One-pot Hydrothermal Synthesis of ZnO Microspheres/Graphene Hybrid and its Electrochemical Performance

Ye Lin<sup>1</sup>, Hongdong Liu<sup>1,\*</sup>, Zhongli Hu<sup>1</sup>, Rong Hu<sup>1</sup>, Haibo Ruan<sup>1</sup>, Lei Zhang<sup>2,\*</sup>

<sup>1</sup> Research institute for new materials technology, Chongqing university of arts and sciences, Chongqing 402160, PR China

<sup>2</sup> College of life science, Chongqing normal university, Chongqing 401331, PR China

\*E-mail: [lhd0415@126.com](mailto:lhd0415@126.com), [leizhang0215@126.com](mailto:leizhang0215@126.com)

Received: 29 May 2016 / Accepted: 11 July 2016 / Published: 7 August 2016

---

In this paper, the ZnO microspheres/graphene hybrids were successfully prepared from zinc acetate and GO aqueous solution by a facile one-pot hydrothermal method without any surfactant. The as-synthesized samples were characterized by X-ray diffraction (XRD), field emission scanning electron microscope (FESEM), thermogravimetric (TGA) analysis, nitrogen adsorption/desorption isotherms and pore size distribution. When evaluated as anode material for lithium ion batteries, it delivered a high initial discharge capacity of 1150 mAh g<sup>-1</sup> and exhibited excellent rate performance at different current densities.

---

**Keywords:** ZnO microspheres/graphene hybrid, anode materials, lithium ion batteries, one-pot hydrothermal.

## 1. INTRODUCTION

Lithium ion batteries (LIBs), as the primary green power sources for electric vehicles, portable electric equipment and other small electrical appliances, have attracted special interest in the scientist owing to their superior stability, high specific energy, long working life and lightweight [1-4]. The demand to enhance the safety and rate performance of LIBs has stimulated the search for the next generation of electrode materials especially the negative electrode materials. Up to date, graphite as the conventional anode material in LIBs is limited due to its low theoretical capacity of 372 mAh g<sup>-1</sup> [5-7]. Carbon materials and metal oxides are the current hot electrode materials, the main use of metal oxides are SnO<sub>2</sub>, transition metal oxides (Fe and Co) and ZnO.

Among the various available transition metal oxide anodes, ZnO with the high theoretical capacity of  $978 \text{ mAh g}^{-1}$  has been considered as a promising candidate because of low cost, facile preparation, environmentally friendly and chemical stability[8, 9]. However, despite these advantages, its poor conductivity, large volume and structure change during the charge/discharge process lead to severe capacity fading and low rate capability[10]. There have been effective approaches reported to solving the aforementioned issues by obtaining unique nanostructured morphologies and compositing with carbon materials[11, 12]. In this regard, nanostructured thin films or particles of ZnO have the obvious advantages of a shorter diffusion path for both electrons and Li-ions, larger electrode-electrolyte contact area and a better accommodation for the strain caused by lithium insertion/desertion[13, 14]. Furthermore, various carbon materials such as amorphous carbon, carbon nanofibers, carbon nanotubes and graphite have been utilized to modify ZnO and enhance the overall conductivity of the electrodes[15, 16]. In recent years, graphene receives considerable attention because of unique 2D structure with excellent electrical, large specific surface area, high mechanical strength, which is beneficial to improve lithium storage performance[17, 18]. The ZnO/graphene composites, including ZnO flower/RGO[19], ZnO nanoparticle/ graphene[20] and ZnO nanosheet/graphene[21] can significantly improve the rate and cycling stability than the pure ZnO anode. The composite presents positive synergistic effects between the metal oxide and the carbon material that could successfully relieve the volume change and improve the electrochemical performance with excellent cycling stability and rate capability[22, 23]. In addition, graphene is as promising substrate loading, coating and weaving nanomaterials for LIBs, resulting in the formation of loose 3D network structure. Unfortunately, the layered graphene sheets can unaffectedly stack into multilayers and lose the advantages of high surface area and high electron mobility[24, 25]. ZnO anchored on the graphene sheets could potentially resolve the problem of graphene stacking.

In this paper, graphene oxide (GO) was successfully synthesized using graphite as raw material, then ZnO microspheres/graphene composites were obtained from zinc acetate and GO aqueous solution by a facile one-pot hydrothermal method without any surfactant. The results improved lithium storage performance of ZnO microspheres/graphene electrodes in LIBs, which showed a potential feasibility for replacing the commercial graphite anodes.

## 2. EXPERIMENTAL

### 2.1. Preparation of grapheme oxide

Graphene oxide was first prepared by the natural graphite using the modified Hummers' method. Typically, graphite power (2 g) and sodium nitrate (1 g) were dissolved in concentrated sulphuric acid (46 mL) under stirring constantly in an ice water bath (0-3 °C) for 15 min. Then, potassium permanganate (6 g) was gradually added into the above solution keeping magnetic stirring for 24 h. Next, a certain amount of  $\text{H}_2\text{O}_2$  aqueous solution and de-ionized water was added into the above mixture over 1 h with stirring to get yellow-brown solution. After that, the suspension was washed and centrifuged with de-ionized water until the pH value of the filtrate was neutral and dried under vacuum at 80 °C for overnight. Finally, the dried graphite oxide was heated at 1000 °C under Ar to get graphene oxide.

## 2.2. Preparation of ZnO microspheres/graphene hybrid

ZnO microspheres/graphene composite was synthesized by a facile one-pot hydrothermal method. The mixture of 20 mg of graphene oxide and 200 mg of Zn(AC)<sub>2</sub> were dispersed in 45 mL of ethylene glycol with ultrasonication for 30 min. Subsequently, 20  $\mu$ L of hydrazine hydrate was slowly added into the mixture with stirring and then transferred into a 50 mL Teflon-lined stainless steel autoclave, sealed tightly, and heated at 180 °C for 16 h. After cooling naturally in air, the product was collected by washing and centrifuging with de-ionized water and ethanol for several times, and then dried under vacuum.

## 2.3. Characterization

The phase structure of the samples were characterized by German Bruker ASX D8 focus type X-ray diffraction powder equipped with Cu/K $\alpha$  radiation ( $\lambda=0.15406$  nm), the collection angles were set to 10 to 60 ° with a scanning rate of 4° min<sup>-1</sup>. N<sub>2</sub> adsorption/desorption isotherms and pore size distribution were measured by ASAP 2020 M, the morphology and structure of the samples were investigated by FESEM, NOVA 400 field emission scanning electron microscope. TGA curves were carried out by TGA/DSC1/1100LF thermogravimetric analyzer in Sweden Mettler company to analysis the content of ZnO.

## 2.4. Electrochemical measurements

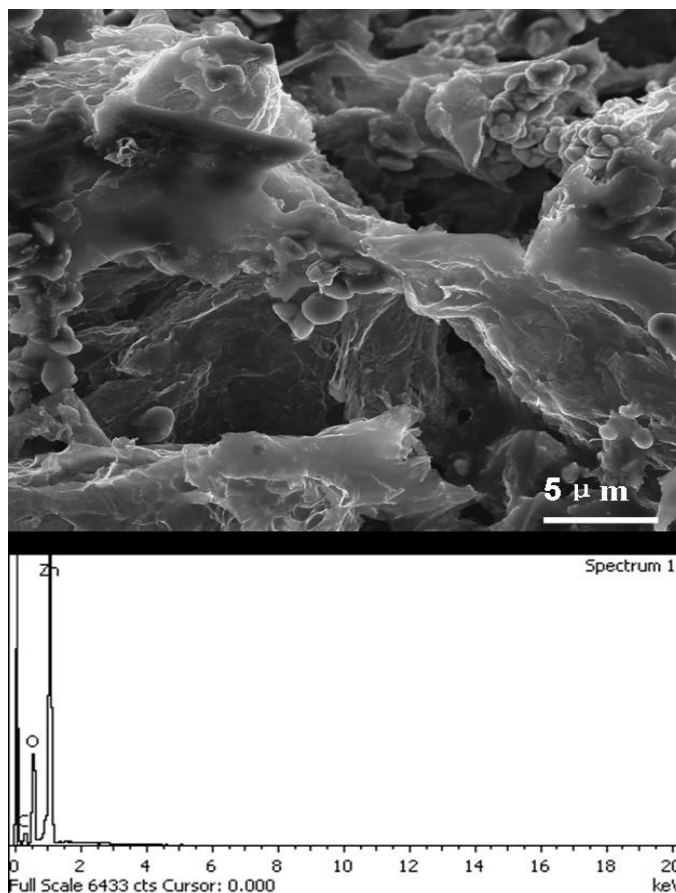
CR2032 coin cells were assembled in an argon-filled glove box for electrochemical measurements. Firstly, 80 wt% as-prepared samples were mixed with 10 wt% acetylene black as conductive agent and 10 wt% polyvinylidene fluoride (PVDF) as binder in 1-methyl-2-pyrrolidinone (NMP) solvent to prepare the electrode slurry. Then the slurry was uniformly coated on the copper foil, dried in vacuum at 100 °C for overnight to get the working electrodes. It was a three-electrode system that the pure lithium sheet worked as the counter and reference electrode and above slurry as the working electrodes. The electrolyte was the mixture of 1 M LiPF<sub>6</sub> in ethylene carbonate (EC) and dimethyl carbonate (DMC) at volume ratio of 1:1. A Celgard 2400 microporous polypropylene film was used as the separator.

Cyclic voltammetry (CV) were carried out at scan rate of 0.05 mV/s and Electrochemical impedance spectral measurements (EIS) were performed in the frequency range from 100 kHz to 0.01Hz. Both them were measured on a CHI 760E electrochemistry workstation. Galvanostatic charge-discharge cycles were tested on a Battery Testing System (Neware BTS-610) between 0 and 3V at the different current densities.

## 3. RESULTS AND DISCUSSION

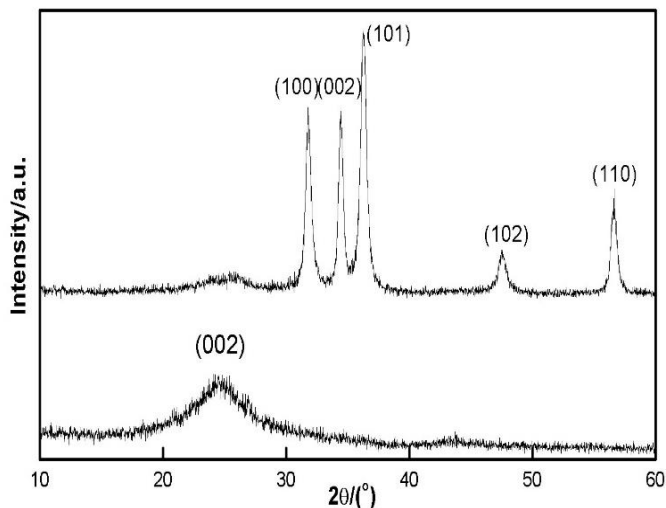
Figure 1 showed the morphology and structure of ZnO microspheres/graphene hybrid characterized by FESEM and EDS. Form the FESEM pattern, two dimensional (2D) flake graphene

with thin sheet structure was observed, the ZnO microspheres with an average size of 2.0  $\mu\text{m}$  were anchored onto the surface of graphene sheets, which significantly resolved the problem of graphene stacking. Actually, the ZnO microspheres and (2D) flake graphene formed a unique 3D network structure which could play an important role in shorting the transmission path of electron and buffering the volume changes during the charge/discharge processes. The EDS spectrum of samples clearly showed the existence of three elements C, O and Zn, indicating the ZnO microspheres/graphene hybrid prepared by One-pot hydrothermal synthesis was free from elemental impurities.



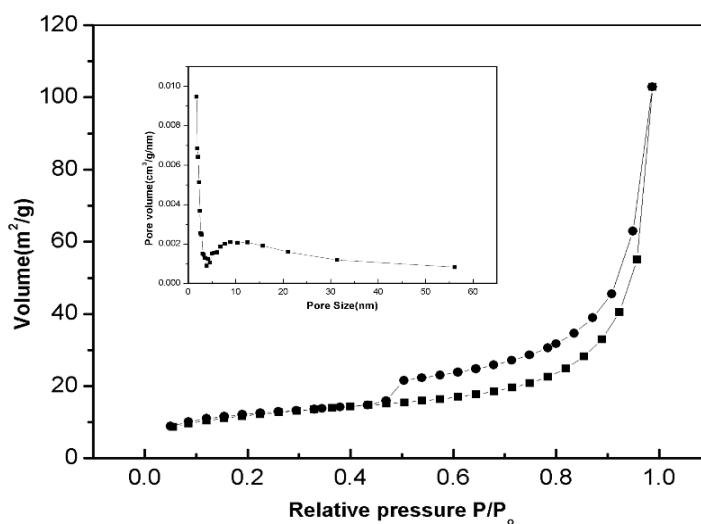
**Figure 1.** FESEM and EDS pattern of the ZnO microspheres/graphene hybrid

The crystal structures of GO and ZnO microspheres/graphene hybrid were further studied by powder X-ray diffraction in Figure 2. From the figure 2 can be seen that the (001) diffraction peak of layered GO after obtaining composite almost disappeared and the weak (002) diffraction peak of GO at about  $24^\circ$  still existed [26, 27]. This result implied that ZnO microspheres inserted GO layered-sheet without changing the overall structure of GO. In addition, five ZnO diffraction peaks assigned to (100), (002), (101), (102), and (110) planes were obviously observed, in  $32^\circ$ ,  $34^\circ$ ,  $36.5^\circ$ ,  $48.2^\circ$ , and  $56.4^\circ$ , respectively. These diffraction peaks can be well-indexed to wurtzite-type hexagonal phase ZnO without any impurities, indicating ZnO excellent crystallinity properties.



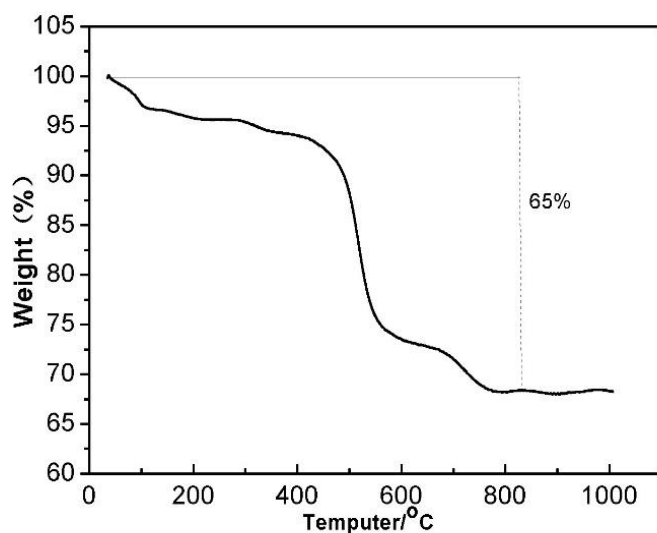
**Figure 2.** XRD patterns of the ZnO microspheres/graphene hybrid

Figure 3 was the N<sub>2</sub> adsorption/desorption isotherms of composite materials. Inset is pore size distribution. Nitrogen adsorption measurements were used to determine the surface area and pore size of the hybrid. The isotherms can be attributed to type H3 according to IUPAC classification, indicating the mesoporous structure of the hybrid. The illustration revealed the composite had a pore diameter about 5.0 nm, which confirmed the mesoporous structure. The specific surface area of the composite was 41.6 m<sup>2</sup>/g, and pore volume was 0.159 cm<sup>3</sup>/g, according to the nitrogen adsorption/desorption isotherms. Therefore, it could be concluded that the hybrid had a hierarchically porous structure, which is beneficial for the transport of lithium ions and the electrolyte in LIBs during the charge/discharge process.



**Figure 3.** N<sub>2</sub> adsorption/desorption isotherms of the ZnO microspheres /graphene hybrid, inset is pore size distribution

In order to determine the content of ZnO microspheres in the composite, the thermogravimetry (TG) analysis of the composite was carried out from 0-1000 °C in air. The TGA curve in Figure 4 showed a weight loss caused by the decomposition of graphene in air. In the process of preparing GO, graphite would produce some oxygen-containing functional groups and defects, due to the oxidation of acid, which caused the weight loss of GO at different temperatures in the high temperature combustion process. The combustion temperature of the oxygen-containing functional groups and graphite were about 580 °C and 720 °C, respectively. The results revealed that the weight percentage of ZnO microspheres in the hybrid was measured to be about 65 %.



**Figure 4.** TGA curve of the ZnO microspheres/graphene hybrid

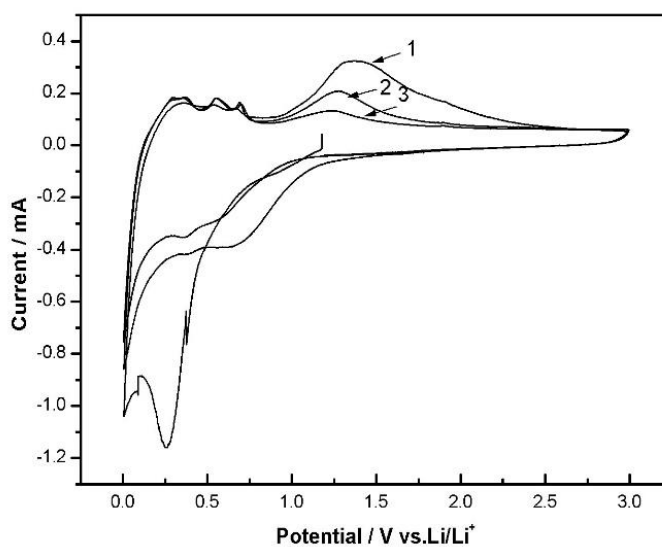


**Figure 5.** CV curves of the ZnO microspheres/graphene hybrid at a scan rate of 0.05 mVs<sup>-1</sup>.

To display the electrochemical properties of ZnO microspheres/graphene hybrid as anode materials in LIBs, cyclic voltammetry (CV) and galvanostatic charge-discharge measurements were conducted. Figure 5 is the CV curves of the ZnO microspheres/graphene hybrid anode for the 1st, 2nd and 3th cycles in the potential range from 0 V to 3 V (vs. Li<sup>+</sup>/Li) at a scan rate of 0.05 mV s<sup>-1</sup>. In the first cathodic scan, there was a strong reduction peak at around 0.01 V identified to the insertion of Li into RGO, suggesting the electrochemical activation of RGO for lithium storage. A another sharp reduction peak at 0.25 V might be ascribed to the reduction of ZnO to Zn[8, 28, 29], the formations of Li-Zn alloy and a solid electrolyte interface (SEI) layer on the electrode surface. The main component of (SEI) layer was an organic layer consisting of ethylene, LiF, Li<sub>2</sub>CO<sub>3</sub> and ROCO<sub>2</sub>Li. The four oxidation peaks located at about 0.26 V, 0.48 V, 0.62 V, and 1.26 V in the first anodic scan was related to the extraction of Li from RGO, the oxidation of Zn to ZnO[21, 26], the multi-step de-alloying process of Li-Zn alloy, the decomposition of (SEI) layer and Li<sub>2</sub>O, respectively. In the subsequent cycles, the cathodic peaks shifted due to the structure modification[30], but the anodic peaks overlapped very well, suggesting high reversibility and good stability. This was because that ZnO composited with graphene to enhance the electrochemical performance by short the path of the insertion and extraction of Li. The insertion/extraction reaction of lithium ion into ZnO microspheres as below:

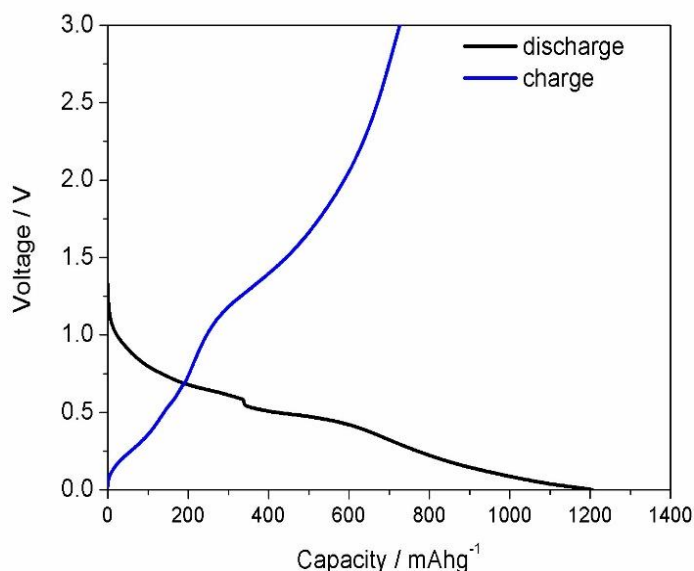
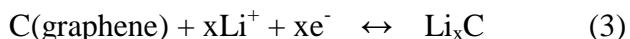


**Figure 6.** Charge/discharge profiles of the ZnO microspheres/graphene hybrid at the current density of 80 mA g<sup>-1</sup>

Figure 6 exhibited the galvanostatic discharge-charge profiles of the hybrid at the current density of 80 mA g<sup>-1</sup> in the voltage of 0~3.0 V. The voltage plateaus was in good agreement with the CV results. The first initial discharge capacity was 1150 mAh g<sup>-1</sup> much higher than the theoretical

value of  $978 \text{ mAh g}^{-1}$ . However, the charge capacity dramatically decreased to  $725 \text{ mAh g}^{-1}$ . This high irreversible specific capacity was believed to originate from the electrolyte decomposition in the low-potential region and (SEI) layer formation on the electrode surface[31, 32]. It could be better in the subsequent cycles, which would improve Li ion storage capacity and enhance the reversible performance.

Furthermore, the rate performance of the hybrid was investigated by increasing the current densities from  $80$  to  $320 \text{ mA g}^{-1}$  in figure 7. The first discharge capacity reached to  $725 \text{ mAh g}^{-1}$  at a current density of  $80 \text{ mA g}^{-1}$ . Then, the capacity quickly decreased with the increase of the current density. It reached to  $270 \text{ mAh g}^{-1}$  after 10 cycles at a current density of  $160 \text{ mA g}^{-1}$  and  $200 \text{ mAh g}^{-1}$  at a current density of  $320 \text{ mA g}^{-1}$ , which remained 27.6 %, comparing to the initial specific capacity. The decreased capacity at high rate was maybe due to the slow kinetics.

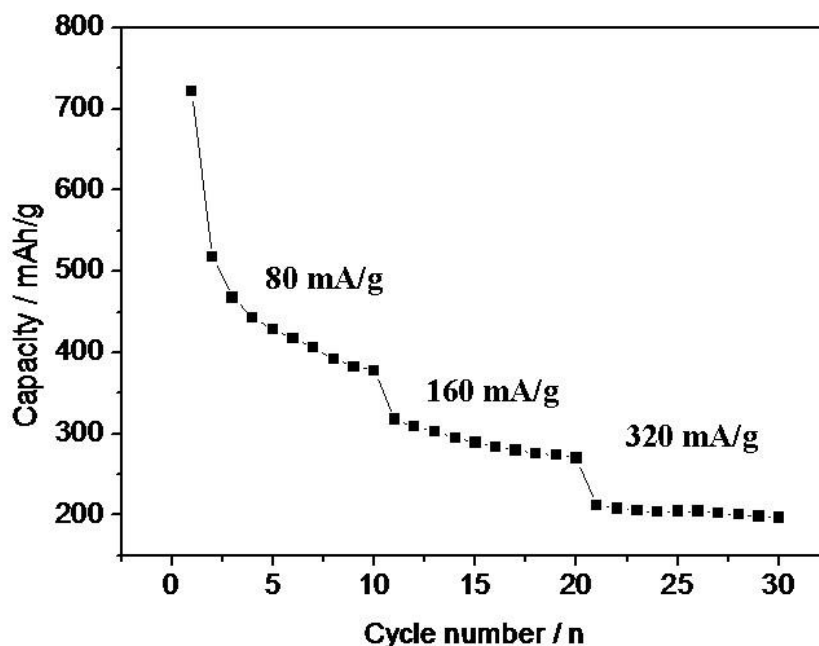


Figure 7. Rate capability of the ZnO microspheres/graphene hybrid.

#### 4. CONCLUSION

In summary, the ZnO microspheres/graphene hybrid was successfully prepared from zinc acetate and GO aqueous solution by a facile one-pot hydrothermal method without any surfactant. The ZnO microspheres with an average size of  $2.0 \mu\text{m}$  were anchored onto the matrix of graphene sheets to form the ZnO/graphene hybrid. Such loose 3D network structure established by GO sheets could efficiently relieve the volume change and enhance the electrode conductivity, which was attributed to the positive synergistic effects between the metal oxide and the carbon material. When adopted as anode material for LIBs, it delivered a high initial discharge capacity of  $1150 \text{ mAh g}^{-1}$  and exhibited excellent rate performance at different current density. Furthermore, the current synthesis strategy was

simple, effective and it may be extended to prepare other various functional hybrid materials applications in LIBs.

#### ACKNOWLEDGEMENTS

This work was financially supported by Basic and Frontier Research Program of Chongqing Municipality (cstc2015jcyjA90020) and (cstc2014jcyjA10063), Scientific and Technological Research Program of Chongqing Municipal Education Commission (KJ1501101), (KJ1500323) and (KJ1501116), China Postdoctoral Science Foundation (2015M582499), Postdoctoral special Foundation of Chongqing (Xm2015064) and Project of Chongqing Normal University (14XY025) and (14XLB004), and National Natural Science Foundation of China (51502030).

#### References

1. K. Chang, D. Geng, X. Li, J. Yang, Y. Tang, M. Cai, R. Li, X. Sun, *Advanced Energy Materials*, 3 (2013) 839-844.
2. M. Choi, S.K. Koppala, D. Yoon, J. Hwang, S.M. Kim, J. Kim, *Journal of Power Sources*, 309 (2016) 202-211.
3. X. Fan, J. Shao, X. Xiao, L. Chen, X. Wang, S. Li, H. Ge, *Journal of Materials Chemistry A*, 2 (2014) 14641.
4. J. Guo, L. Ma, X. Zhang, Y. Zhang, L. Tang, *Materials Letters*, 118 (2014) 142-145.
5. X. Jiang, X. Yang, Y. Zhu, Y. Yao, P. Zhao, C. Li, *J. Mater. Chem. A*, 3 (2015) 2361-2369.
6. H.-W. Kim, D.J. Lee, H. Lee, J. Song, H.-T. Kim, J.-K. Park, *Journal of Materials Chemistry A*, 2 (2014) 14557.
7. C. Liang, T. Zhai, W. Wang, J. Chen, W. Zhao, X. Lu, Y. Tong, *Journal of Materials Chemistry A*, 2 (2014) 7214.
8. X. Chen, Y. Huang, X. Zhang, C. Li, J. Chen, K. Wang, *Materials Letters*, 152 (2015) 181-184.
9. J. Dai, M. Wang, M. Song, P. Li, C. Zhang, A. Xie, Y. Shen, *Scripta Materialia*, 112 (2016) 67-70.
10. Y. Sun, H. Guo, W. Zhang, T. Zhou, Y. Qiu, K. Xu, B. Zhang, H. Yang, *Ceramics International*, 42 (2016) 9648-9652.
11. R. Guo, W. Yue, Y. An, Y. Ren, X. Yan, *Electrochimica Acta*, 135 (2014) 161-167.
12. Y. Liu, Y. Li, M. Zhong, Y. Hu, P. Hu, M. Zhu, W. Li, Y. Li, *Materials Letters*, 171 (2016) 244-247.
13. X. Wang, L. Huang, Y. Zhao, Y. Zhang, G. Zhou, *Nanoscale Res Lett*, 11 (2016) 37.
14. S. Zhang, S.-L. Zhou, L.-N. Zhang, D.-H. Wu, S. Du, C.-T. Chang, *Materials Letters*, 171 (2016) 263-267.
15. S. Li, Y. Xiao, X. Wang, M. Cao, *Phys Chem Chem Phys*, 16 (2014) 25846-25853.
16. M. Yu, A. Wang, Y. Wang, C. Li, G. Shi, *Nanoscale*, 6 (2014) 11419-11424.
17. M. Liu, J. Sun, *Journal of Materials Chemistry A*, 2 (2014) 12068.
18. J. Zhou, H. Xiao, B. Zhou, F. Huang, S. Zhou, W. Xiao, D. Wang, *Applied Surface Science*, 358 (2015) 152-158.
19. S. Xu, L. Fu, T.S.H. Pham, A. Yu, F. Han, L. Chen, *Ceramics International*, 41 (2015) 4007-4013.
20. N. Song, H. Fan, H. Tian, *Applied Surface Science*, 353 (2015) 580-587.
21. Y. Huang, X. Chen, K. Zhang, X. Feng, *Ceramics International*, 41 (2015) 13532-13540.
22. Y. Zhao, H. Li, Y. Zhang, H. Xie, F. Yin, *Int.J. Electrochem. Sci.*, 11 (2016)3179-3189
23. J. Hwang, H. Lim, Y. Sun, K. Suh, *Journal of Power Source*, 244 (2013) 538-543
24. Y. Peng, J. Ji, D. Chen, *Applied Surface Science*, 356 (2015) 762-768.
25. W.-H. Hu, R. Yu, G.-Q. Han, Y.-R. Liu, B. Dong, Y.-M. Chai, Y.-Q. Liu, C.-G. Liu, *Materials Letters*, 161 (2015) 120-123.
26. Y.-Z. Liu, Y.-F. Li, Y.-G. Yang, Y.-F. Wen, M.-Z. Wang, *Scripta Materialia*, 68 (2013) 301-304.
27. K. Zhao, W. Gu, L. Zhao, C. Zhang, W. Peng, Y. Xian, *Electrochimica Acta*, 169 (2015) 142-149.

28. Z. Zhang, L. Ren, W. Han, L. Meng, X. Wei, X. Qi, J. Zhong, *Ceramics International*, 41 (2015) 4374-4380.
29. L. Zhang, J. Zhang, Y. Liu, P. Zheng, X. Yuan, S. Guo, *Materials Letters*, 165 (2016) 165-168.
30. M. Yu, D. Shao, F. Lu, X. Sun, H. Sun, T. Hu, G. Wang, S. Sawyer, H. Qiu, J. Lian, *Electrochemistry Communications*, 34 (2013) 312-315.
31. J. Wu, C. Chen, Y. Hao, C. Wang, *Colloids and Surfaces A: Physicochemical and Engineering Aspects*, 468 (2015) 17-21.
32. C.-T. Hsieh, C.-Y. Lin, Y.-F. Chen, J.-S. Lin, *Electrochimica Acta*, 111 (2013) 359-365.

© 2016 The Authors. Published by ESG ([www.electrochemsci.org](http://www.electrochemsci.org)). This article is an open access article distributed under the terms and conditions of the Creative Commons Attribution license (<http://creativecommons.org/licenses/by/4.0/>).